



Published in final edited form as:

*Circ Res.* 2016 January 22; 118(2): 203–215. doi:10.1161/CIRCRESAHA.115.307399.

## Intact Heart Loose Patch Photolysis Reveals Ionic Current Kinetics During Ventricular Action Potentials

Josefina Ramos-Franco<sup>1</sup>, Yuriana Aguilar-Sanchez<sup>2</sup>, and Ariel L. Escobar<sup>3</sup>

<sup>1</sup>Department of Molecular Biophysics and Physiology, Rush University Medical Center, Chicago, IL

<sup>2</sup>Quantitative Systems Biology Program, School of Natural Sciences, University of California, Merced, Merced CA

<sup>3</sup>Biological Engineering and Small Scale Technologies Program, School of Engineering, University of California, Merced, Merced, CA

### Abstract

**Rationale**—Assessing the underlying ionic currents during a triggered action potential (AP) in intact perfused hearts offers the opportunity to link molecular mechanisms with pathophysiological problems in cardiovascular research. The developed Loose Patch Photolysis (LPP) technique can provide striking new insights into cardiac function at the whole heart level during health and disease.

**Objective**—To measure transmembrane ionic currents during an AP in order to determine how and when surface  $\text{Ca}^{2+}$  influx that triggers  $\text{Ca}^{2+}$  induced  $\text{Ca}^{2+}$  release (CICR) occurs and how  $\text{Ca}^{2+}$  activated conductances can contribute to the genesis of AP phase 2.

**Methods and Results**—LPP allows the measurement of transmembrane ionic currents in intact hearts. During a triggered AP, a voltage-dependent  $\text{Ca}^{2+}$  conductance was fractionally activated (dis-inhibited) by rapidly photo-degrading nifedipine, the  $\text{Ca}^{2+}$  channel blocker. The ionic currents during a mouse ventricular AP showed a fast early component and a slower late component. Pharmacological studies established that the molecular basis underlying the early component was driven by an influx of  $\text{Ca}^{2+}$  through the L-type channel,  $\text{Ca}_v 1.2$ . The late component was identified as a  $\text{Na}^+$ - $\text{Ca}^{2+}$  exchanger (NCX) current mediated by  $\text{Ca}^{2+}$  released from the sarcoplasmic reticulum (SR).

**Conclusions**—The novel LPP technique allowed the dissection of transmembrane ionic currents in the intact heart. We were able to determine that during an AP L-Type  $\text{Ca}^{2+}$  current contributes to phase 1 while NCX contributes to phase 2. In addition, LPP revealed that the influx of  $\text{Ca}^{2+}$  through L-type  $\text{Ca}^{2+}$  channels terminates due to voltage-dependent deactivation and not by  $\text{Ca}^{2+}$  dependent inactivation, as commonly believed.

---

**Address correspondence to:** Dr. Ariel L. Escobar, Biological Engineering and Small Scale Technologies, School of Engineering, University of California, Merced, Merced, CA, USA, Tel: 209-216-4618, Fax: 209-216-4108, aescobar4@ucmerced.edu.

### DISCLOSURE

None.

## Keywords

Ventricular action potentials; excitation-contraction coupling; calcium signaling; L-type calcium current; Na<sup>+</sup>/Ca<sup>2+</sup> exchange

---

## INTRODUCTION

In mammalian hearts, the complex nature of electrocardiographic signals is critically defined by the timing of the action potential (AP) at the different layers within the ventricular wall<sup>1</sup>. The ventricular AP has 5 distinguishable temporal phases driven by the activation of ionic currents<sup>2,3</sup>. In particular, the duration and amplitude of AP phase 2 is considered to be critical for excitation-contraction coupling (ECC) since it is thought to determine the magnitude of Ca<sup>2+</sup> influx through L-type Ca<sup>2+</sup> channels<sup>4,5</sup>, which predominantly occurs during this phase<sup>5,6</sup>. However, the time course of APs are highly heterogeneous within different areas<sup>7,8,9</sup> and layers<sup>10,11,12</sup> of the ventricles. These heterogeneities are driven by non-homogenous distribution of ionic channels<sup>13,14</sup> that produce currents underlying the AP morphology. Furthermore, diverse mammalian species display different AP time courses, indicating that the contribution of specific ionic conductances defining the AP in one species cannot be extrapolated to another one.

Much of our knowledge about the ionic currents underlying the AP has been from measurements on enzymatically dissociated ventricular cardiac myocytes. A standard method is to record APs in current clamp mode and then voltage clamping the myocytes using the recorded AP waveform<sup>15,16,17</sup> (AP voltage clamp). The different ionic components can then be dissected using pharmacological tools. This approach has generated a great deal of knowledge, but it has several drawbacks and limitations. For example, the exact ventricular area and layer from where the tested dissociated myocytes originated is largely unknown. The electrical, metabolic and mechanical coupling within the ventricular syncytium (and its influence on the AP) is lost when cells are dissociated. Furthermore, ionic currents in isolated myocytes are usually recorded at room (not physiological) temperature and in the presence of exogenous intracellular Ca<sup>2+</sup> buffers to help sustain cell viability. We developed Loose Patch Photolysis (LPP) to overcome these obstacles. It allowed us for the first time to simultaneously measure transmembrane currents ( $i_m$ ) during a triggered AP in an intact heart by activating or inhibiting ionic conductances using photosensitive compounds.

We recently reported<sup>7</sup> that, in mouse epicardium, AP phase 2 occurs at a membrane potential ( $V_m$ ; more negative than -40 mV) at which L-type Ca<sup>2+</sup> channels are closed<sup>18</sup>. This finding spurred two questions that can be answered with our newly-developed technique. These questions are: 1) If Ca<sup>2+</sup> does not enter the cell during phase 2, what ionic conductance is responsible for phase 2 in mouse epicardium? and 2) When does the Ca<sup>2+</sup> influx that triggers Ca<sup>2+</sup> induced Ca<sup>2+</sup> release (CICR) occur?

Here, we used LPP to definitively show that, the Ca<sup>2+</sup> influx that triggers CICR occurs during AP phase 1 in mouse epicardium and AP phase 2 is due to Na<sup>+</sup>-Ca<sup>2+</sup> exchanger (NCX) mediated inward current driven by Ca<sup>2+</sup> release from the sarcoplasmic reticulum

(SR), not the L-type  $\text{Ca}^{2+}$  channel. The results presented here challenge the long-standing concept that, in all mammals, the AP phase 2 is responsible for triggering CICR.

Finally, our finding that  $\text{Ca}^{2+}$  influx that triggers CICR occurs during AP phase 1 opens the possibility that this scenario could also occur in the epicardium of other mammals including humans that have a strong “spike and dome” AP morphology. Our state-of-the-art LPP approach is a new powerful tool that can be used to define the properties of ionic currents in the intact heart during pathophysiological situations like ischemia or arrhythmias, where intact heart recordings are essential.

## METHODS

### Heart preparation

Animals used in this study (male Balb/c, 3–7 weeks-old) were maintained in accordance with the National Institutes of Health Guide for the Care and Use of Laboratory Animals (NIH Publication No. 85–23, Revised 1996) and were euthanized by cervical dislocation. This protocol was approved by the Institutional Animal Care and Use Committee of the University of California Merced (# 2008–201). Hearts were removed and cannulated onto a custom-design recording chamber attached to a Langendorff apparatus and continuously perfused at a rate of 1 mL/min with Tyrode solution. Tyrode consists of (in mM): 140 NaCl, 5.4 KCl, 2  $\text{CaCl}_2$ , 1  $\text{MgCl}_2$ , 0.33  $\text{Na}_2\text{HPO}_4$ , 10 HEPES, 10 glucose, pH=7.4. The temperature of the solution outside the heart was controlled with a Peltier unit that allowed us to maintain the heart at *quasi* physiological temperatures during the whole experiment. All solutions were equilibrated with 100%  $\text{O}_2$ . Hearts were paced at the apex, at 6 Hz using an optically isolated current stimulator (Isostim, WPI, Sarasota, FL) at 32°C.

### Fluorophore loading

Rhod-2 and X-Rhod-5F AM were used to measure myoplasmic  $\text{Ca}^{2+}$  concentration and Di-8-ANEPPS to record the membrane potential. The dyes were dissolved in DMSO (Sigma, St Louis, MO) with 2.5% Pluronic, the stock solution was finally diluted in Tyrode solution to reach a final dye concentration of 45  $\mu\text{M}$  for the  $\text{Ca}^{+2}$  indicators and 1.5  $\mu\text{M}$  for the potentiometric dye. Perfusion with dyes started after the spontaneous heart rate became regular. After 30 min of perfusion at room temperature, the solution containing the fluorescent dye was switched to Tyrode solution and temperature was increased to 32°C within 10 min. In all the experiments, the hearts were perfused with 10  $\mu\text{M}$  blebbistatin to reduce the motion. All the recordings were performed at the epicardial layer. All the dyes were obtained from Life Technologies (Carlsbad, CA) and additional drugs and salts from Sigma (St Louis, MO).

### Pulsed Local Field Fluorescence Microscopy (PLFFM) setup

PLFFM has been extensively described elsewhere<sup>19,20</sup>. Briefly, the excitation light source was obtained from a green (532 nm) Yag laser. The light pulses were focused by an objective into a small (200  $\mu\text{m}$  dia, 0.67 NA) multimode optical fiber. Emitted light was carried back through the same fiber, filtered and focused on an avalanche photodiode (Perkin Elmer, Waltham, MA). The recordings were obtained by gently placing one end of fiber on

the tissue to immobilize the fiber optic relative to the heart surface. This procedure greatly attenuated motion artifacts.

Additionally, intracellular membrane potential was also recorded with sharp glass microelectrodes filled with 3 M KCl and connected to an electrometric amplifier (WPI, Sarasota, FL). Data acquisition was performed with a multifunction acquisition board (National Instruments, Austin, TX) controlled by a custom-designed, G-based software program (LabVIEW).

### Loose Patch Photolysis (LPP) setup

This novel technique allowed us to record ionic currents during a triggered epicardial AP. The system is a combination of three major elements (Fig. 1S): loose patch recordings<sup>21,22</sup>, local field optical measurements<sup>19,20</sup> and fiber optic laser driven flash photolysis<sup>23,24,25,26,27</sup>. The first component, a dual patch clamp allowed us to voltage clamp at the same potential the interior of a macro-patch pipette and the surrounding bath. This configuration equalized both potentials in order to eliminate the pipette seal leak current. As illustrated in Fig. 1A

$$V_o = -R_f \cdot i_p = R_f \cdot (i_{seal} + i_m) \quad (1)$$

where  $V_o$  and  $R_f$  are the current-to-voltage converter output voltage and feedback resistor, respectively,  $i_p$  is current flowing through the patch pipette,  $i_{seal}$  is leak current through the loose seal and  $i_m$  is membrane current. Usually, because of a poor electrical seal between the pipette and the tissue

$$i_{seal} \gg i_m \quad (2)$$

then

$$i_p = i_m + i_{seal} = \frac{V_m}{r_m} + \frac{V_A - V_{bath}}{r_{seal}} \quad (3)$$

where  $V_m$  is the membrane potential,  $r_m$  is the membrane resistance,  $V_A$  is the potential inside the pipette,  $V_{bath}$  is the extracellular potential outside the heart and  $r_{seal}$  is the seal resistance.

If

$$V_A = V_{bath} \Rightarrow i_{seal} = 0 \quad (4)$$

therefore

$$V_o = -R_f \cdot i_m \quad (5)$$

Thus, voltage clamping the bath and the pipette at the same potential allowed us to directly evaluate the membrane current during an AP.

The second component, a local field fiber optic positioned inside the patch pipette was used to optically record the AP inside the pipette. As seen in Fig. 1B, the currents recorded during an AP after “sealing” the patch pipette against the tissue displayed a complex behavior. The complexity of this signal relies on the fact that the recorded membrane current is the summatory of the total ionic current plus a capacitive current. Indeed,

$$i_m = i_c + \sum i_i \quad (6)$$

where  $i_c$  is the capacitive current and  $i_i$  is each of the individual ionic currents occurring during the AP. The capacitive current will depend on the rate at which the membrane potential changes below the pipette. So,

$$i_m = C_m \frac{dV_m}{dt} + \sum i_i \quad (7)$$

where  $C_m$  is the membrane capacitance. Since we are interested in the ionic currents the previous equation can be rearranged as follows:

$$\sum i_i = i_m - C_m \frac{dV_m}{dt} \quad (8)$$

Thus, to evaluate the total ionic current, the membrane current and the membrane potential need to be evaluated at the same site. This was performed by optically recording the membrane potential at the patch pipette with a local field optical fiber positioned inside the pipette (Fig. 1C). The resting membrane potential and the amplitude of the optically recorded AP were calibrated with the aid of an electrical signal obtained with a sharp microelectrode positioned very close to the patch pipette (Fig. 1C).

The third component, a flash photolysis system, allowed us, by the use of light-sensitive drugs, to fractionally change the number of ion channels and/or the open probability of those channels within the patch. For example,  $\text{Ca}^{2+}$  currents can be “activated” (*i.e.*, relieved from partial block) by the photolysis of dihydropyridines (e.g., nifedipine<sup>26,27</sup>) inside the loose patch pipette. Nifedipine partial blockade was locally relieved by UV illumination generated by a DPSS UV laser (355 nm) (DPSS Lasers Inc., Santa Clara, CA). UV light was optomechanically shuttered for 1–40 ms and applied through either a quartz fiberoptic positioned inside or by an additional quartz multimode fiber positioned outside the patch pipette. The pipettes have a tip diameter of 250  $\mu\text{m}$  and the optical fiber 200  $\mu\text{m}$  (depth of field  $\sim$  30  $\mu\text{m}$ ) making it possible to record currents from 25 to 50 myocytes. Using this procedure, we were able to record membrane currents (capacitive and ionic) during the AP before and after the UV flash. The subtraction of the resulting currents before and after the UV flash allowed us to dissect specific ionic currents (see Results).

Data were recorded with an acquisition system Digidata 1440A (Molecular Devices, Sunnyvale, CA) using pClamp 10 software. Fluorescence, membrane potential and currents were always recorded from the left ventricular epicardium.

## Statistical analysis

Data are expressed as means  $\pm$  SE; statistical significance was tested using ANOVA. The difference was considered to be significant if the value of P was  $<0.05$ .

## RESULTS

### Recording transmembrane currents during a triggered AP

Measuring ionic currents in multicellular preparations has been challenging both in application and interpretation because of difficulties to spatially voltage clamp the tissue and the impossibility of obtaining high-resistance electrical seals using giant patch pipettes.

To overcome these problems, we developed the novel LPP technique that allowed us to measure  $i_m$  during a triggered physiological AP. This was achieved by voltage clamping to the same potential the interior of a giant patch pipette and the bath where the heart was immersed. This procedure eliminates the seal current ( $i_{seal}$ ) by zeroing the potential difference between the pipette and the bath. A scheme of the system is shown in Fig. 1A. With the bath potential clamped to  $V_A$ ,  $i_{seal}$  is eliminated, and the entire remaining current flowing through the pipette will be the current flowing across the plasma membrane ( $i_m$ ) (see Methods). Fig. 1B illustrates a membrane current induced by an AP and recorded in a loose seal before and after the patch pipette was gently pressed against the ventricular epicardial layer. The recorded signal presents a complex biphasic behavior composed of the stimulus artifact (large downward spike) and a compound current waveform that includes capacitive and ionic currents. As described in Methods to evaluate the capacitive component, the  $V_m$  during an AP needs to be recorded in the same location as  $i_m$ . This was achieved by, loading the heart with the potentiometric dye Di-8-ANEPPS and positioning a PLFFM optical fiber inside the recording glass pipette (Fig. 1C). Traces of optically and electrically recorded APs in conjunction with  $i_m$  are shown in Fig. 1D. The optically recorded AP allowed us to simultaneously assess the total  $i_m$  in conjunction with the  $i_c$  in an intact heart assuming that the membrane specific capacitance is  $1\mu\text{F}/\text{cm}^2$  (Fig. 1E).

### Dissecting transmembrane currents during an AP

Although the loose patch allowed us to record  $i_m$  locally during an AP, it is problematic to selectively change the activity of a specific ionic conductance (e.g., L-type  $\text{Ca}^{2+}$  current) in the patch. The traditional approach of separating the component conductances using voltage-clamp approaches cannot be adopted, because neither the patch membrane nor the cell can be voltage-clamped *in situ*. Changing the pipette potential with respect to the bath to activate voltage dependent currents will result in a massive increase in  $i_{seal}$  that will prevent the electrical recording of  $i_m$ . To tackle this problem, we decided to activate an ionic conductance photolytically. This was achieved by perfusing the heart with nifedipine, a well-known L-type  $\text{Ca}^{2+}$  channel blocker. The macroscopic  $\text{Ca}^{2+}$  conductance was then activated by photo-relieving the dihydropyridine partial block (Fig. 2A) with the aid of an additional multimode optical fiber carrying a UV beam (Fig. 2B). To test this concept, we recorded  $V_m$  (electrically) and  $\text{Ca}^{2+}$  transients simultaneously.  $\text{Ca}^{2+}$  transients were used as a reporter of SR  $\text{Ca}^{2+}$  release driven by an influx of  $\text{Ca}^{2+}$  across the plasma membrane. Perfusion of the heart with  $10\mu\text{M}$  nifedipine produced a reduction in the AP duration and an attenuation of

the amplitude of the epicardial  $\text{Ca}^{2+}$  transient with respect to their control without nifedipine (Fig. 2C and 2D). Fig. 2C shows a surprising result. When  $\text{Ca}^{2+}$  influx inhibition was removed locally by the photolysis of nifedipine, no statistically significant changes were observed in the AP time course ( $\text{APD}_{90}$  before flash  $45.2 \pm 2.2$  ms vs.  $\text{APD}_{90}$  after flash  $47.9 \pm 3.6$ ,  $p < 0.05$ ). This result was unexpected. In contrast, the  $\text{Ca}^{2+}$  transient following the flash was dramatically enhanced, demonstrating that the photolysis of nifedipine did have profound effects on EC coupling. One possible reason for the unaltered AP time course is that the  $V_m$  recorded with the microelectrode was not obtained at exactly the same location where nifedipine was photolyzed (the microelectrode was positioned 1 mm away from the photolysis optical fiber). To evaluate this explanation, we performed simultaneous electrical and optical recordings of APs (Fig. 2D). As illustrated in Fig. 2D the local optical recording produced the same surprising result. Local photolysis of nifedipine changed neither the electrically nor the optically recorded AP significantly. This result can be interpreted by the fact that nifedipine photolysis might not have changed the plasma membrane conductance. However, the fact that the  $\text{Ca}^{2+}$  transient was markedly enhanced (Fig. 2C) demonstrates that nifedipine photolysis did enhance  $\text{Ca}^{2+}$  influx. The second interpretation is that the local current produced by  $\text{Ca}^{2+}$  influx through L-Type  $\text{Ca}^{2+}$  channels is not able to impact  $V_m$  perceptibly due to the strong isopotential coupling (electrotonic) imposed by the tissue neighboring the recording area. In other words, despite the increased  $\text{Ca}^{2+}$  influx,  $V_m$  did not change because it was physiologically clamped by the surrounding membrane.

The latter premise was evaluated by recording APs electrically at different distances from the photolysis site. A schematic representation of the experiment is presented in Fig. 3A. Fig. 3B illustrates typical AP recordings obtained before and after the nifedipine photolysis at varying distances from the photolysis site. For each spatial position, the black traces represent three consecutive APs before the UV flash. Upon the application of a UV pulse, it is possible to observe a small but distinct effect on the AP (red traces) repolarization after the flash. Two clear observations can be made. First, although the photolytic pulse induced a subtle change in the AP occurring just after the UV pulse, this effect essentially disappears in the following AP. This could be the result of the rapid rebinding of nifedipine after photolysis due to its continuous perfusion. Second, the closer the microelectrode is positioned with respect to the optical fiber used for photolysis, the larger is the effect on the AP repolarization. In order to quantify the maximum nifedipine-induced effect on the AP repolarization, two consecutive AP traces (before and after the flash at the photolysis site) were subtracted. The differential records obtained at increasing photolysis fluences (density of energy) display an early and a late differential component (traces not shown). The early and late components of this difference correspond to changes in AP phase 1 and phase 2, respectively. Fig. 3C shows the percentile difference

$$\left( \frac{\text{AP}_{\text{after photolysis}} - \text{AP}_{\text{before photolysis}}}{\text{AP}_{\text{after photolysis}}} * 100 \right)$$
 induced by the nifedipine photolysis at different fluences of AP recorded at the center of the photolysis site. The percentile difference in the early differential component is significantly larger than in the late differential component ( $n=5$  hearts). The electrotonic effect was assessed by evaluating the space constant of the epicardial tissue after the nifedipine photolysis. Interestingly, Fig 3D shows the spatial attenuation of the early differential component was more abrupt than for



the late differential component ( $273 \pm 25 \mu\text{m}$  vs  $507 \pm 46 \mu\text{m}$ ). These results suggest that under the fluence range  $< 10 \text{ J/cm}^2$ , the difference in the membrane potential change induced by photolysis is smaller than 4%. Additionally, the larger spatial attenuation of the early differential component was expected because the temporal filtering introduced by the cable properties of the tissue is larger for faster differential components than for slower ones.

The increase in the ionic current that triggers SR  $\text{Ca}^{2+}$  release could be related to changes in the  $V_m$  after the photolysis or due to specific effects on the macroscopic  $\text{Ca}^{2+}$  conductance. As we already showed (Fig. 2 and 3), the effect of photolysis on the AP is negligible. Despite this appearance, it could be possible that the small change in the AP was the result of a large change in two opposing conductances. However, the most likely cause is a change in the nifedipine sensitive current, which could result from changes in the number of available channels and/or an increase in the open probability as a result of the photo-degradation of nifedipine. These various possibilities were tested by recording  $i_m$  and optical APs simultaneously (Fig. 4A). We implemented a protocol in which APs and  $i_m$  were recorded before and after a UV flash. Traces obtained using this protocol are shown in Fig. 4B, followed by the subtraction of those consecutive AP and  $i_m$  traces, Fig 4C. The  $V_m$  subtraction before and after the UV flash indicates that  $V_m$  did not change by photolysis. This result reinforces the idea that the tissue outside the patch is imposing an electrotonic.

Moreover,  $i_c = C_m \frac{dV_m}{dt}$  was canceled during the  $i_m$  subtraction because  $V_m$  did not change with photolysis. The differential ionic current ( $i_m$ ) obtained after subtraction showed a biphasic morphology displaying an early fast component ( $i_{early}$ ) and a late slower ( $i_{late}$ ) component. Thus,  $i_m$  displayed in Fig. 4C represents a nifedipine-sensitive ionic current. This current flows locally in the patch membrane, but scarcely affects the recorded AP due to the electrotonic dominated by the  $V_m$  in the larger surrounding membrane area. Hence the  $i_m$  is recorded during a normal AP that is not significantly altered by the local removal of nifedipine.

Mouse epicardial APs exhibit a phase 2 that is partially mediated by  $\text{Ca}^{2+}$  release from the SR<sup>7</sup>. Fig. 5A illustrates that perfusion with ryanodine (Ry) and thapsigargin (Tg), a combination of drugs that impairs  $\text{Ca}^{2+}$  release from the SR, dramatically reduces AP phase 2. With the novel LPP approach, we are in the unique position to determine which of the two components of the nifedipine-sensitive ionic current is responsible for AP's phase 2.

### Properties of the early and late components of the photolytically activated ionic currents

To dissect which of the ionic currents was underlying phase 2, we decided to explore if  $i_{late}$  (Fig. 5B) was activated by  $\text{Ca}^{2+}$  release from SR. The  $i_{late}$  was significantly reduced ( $89.0 \pm 2.1\%$ ) in hearts treated with Ry plus Tg (Fig. 5C–D) in comparison with the effect of the drugs on  $i_{early}$  ( $15.4 \pm 1.3\%$ ) (Fig. 5D and E). Note that in Fig. 5C, early currents recorded after the flash decrease monotonically in time. This effect is due to nifedipine rebinding to dihydropyridine (DHP) receptor on the photolyzed area. See supplementary Online Figure II.

The ionic nature of  $i_{early}$ , was determined using a pharmacological approach. The heart was perfused with  $\text{CdCl}_2$ , a  $\text{Ca}^{2+}$  channel blocker in the presence of Ry plus Tg to eliminate  $i_{late}$ .



This maneuver reversibly inhibited  $i_{early}$  ( $78.7 \pm 3.2\%$ ) (Fig. 6A and 6B) indicating that voltage-dependent DHP-sensitive  $Ca^{2+}$  channels mediate this kinetic component.

As already shown,  $i_{late}$  is an inward current mediated by SR  $Ca^{2+}$  release. Among several possible candidates, an electrogenic influx of  $Na^+$  through the NCX forward mode seems to be a likely candidate<sup>7,28</sup>. To evaluate this option, we perfused hearts with 10  $\mu$ M SEA0400<sup>29</sup>, an NCX blocker. Fig. 6C shows that SEA0400 has a similar effect on AP phase 2 like Ry plus Tg. To evaluate if the effect of SEA0400 was produced by an impairment of the  $Ca^{2+}$  influx to the cells, we recorded  $Ca^{2+}$  transients. Fig. 6D shows that SEA0400 does not decrease the amplitude of the myocytes'  $Ca^{2+}$  transients but rather induced an increase<sup>30</sup>. This effect was consistent with SEA0400 producing a block of NCX that leads, to an increase in the intra SR  $Ca^{2+}$  content. To further demonstrate that  $i_{late}$  was mediated by a  $Na^+$  influx through NCX, we recorded currents in the presence and absence of SEA0400. A typical trace is shown in Fig. 6E where SEA0400 selectively blocked  $i_{late}$  ( $72 \pm 13\%$ ) without affecting ( $11.6 \pm 3.1\%$ )  $i_{early}$  (Fig. 6F). Together, these results demonstrate that, during an epicardial AP, there is a fast influx of  $Ca^{2+}$  through  $Ca^{2+}$  channels responsible for  $i_{early}$ . Additionally, there is a late influx of  $Na^+$  mediated by SR  $Ca^{2+}$  release activation of NCX forward mode, defining  $i_{late}$ .

Even though the early and fast  $Ca^{2+}$  influx during the AP seems to be responsible for triggering SR  $Ca^{2+}$  release, additional evidence is needed. Assessing if incremental  $Ca^{2+}$  influxes during AP can induce incremental  $Ca^{2+}$  transients strengthened this line of evidence. Experiments testing this idea are presented in Fig. 7A–C, where  $Ca^{2+}$  currents (Fig. 7A) and  $Ca^{2+}$  transients (Fig. 7B) were recorded in the same membrane patch. The idea was to increase the amplitude of the  $Ca^{2+}$  current locally by photolyzing progressively greater fractions of nifedipine on the patch surface using UV laser pulses of increasing energy. The direct linear relationship between  $Ca^{2+}$  current and  $Ca^{2+}$  transient amplitudes (Fig. 7C) allowed us quantify the gain of CICR at the intact heart level, for the first time.

A different approach to evaluate the relationship between  $Ca^{2+}$  influx and  $Ca^{2+}$  release was to analyze the relationship between  $i_{late}$  and  $i_{early}$ . One advantage of this approach is that  $i_{late}$  (NCX forward current) will be proportional to the local dyadic  $Ca^{2+}$  concentration during systole. This approach differs from previous measurements using fluorescence indicators in that they only report the mean average intracellular  $Ca^{2+}$  concentration. Another advantage is that the myocytes' internal  $Ca^{2+}$  buffer capacity is not altered by adding an exogenous buffer as occurs when using a  $Ca^{2+}$  indicator dye. Fig. 7D illustrates currents recorded at different nifedipine photolysis fractions (i.e. different fluences). Fig. 7E shows the peak values of  $i_{late}$  and  $i_{early}$  as a function of the fluence. It is possible to observe that both  $i_{late}$  and  $i_{early}$  saturate as a function of the fluence; indicating that for high fluence values (higher than 16 J/cm<sup>2</sup>) most of the nifedipine has been photolyzed. The relationship between  $i_{late}$  and  $i_{early}$  was plotted in Fig. 7F. This curve showed a predominantly nonlinear behavior in comparison with the one illustrated in Fig. 7C which presents a more linear relationship, possibly due to the additional buffering effect introduced by the  $Ca^{2+}$  indicator. A very interesting finding was that early currents with larger magnitude do not terminate faster than smaller ones (Fig. 7A and D). This idea was specifically evaluated in Fig. 7G–I. Fig 7G illustrates traces at different photolysis-fluences that were normalized to the peak current for

each trace. Every trace displayed the same kinetics for different fluences, suggesting that the magnitude of the current does not impact the current termination. Furthermore, data from 5 different hearts show that the kinetics of relaxation of the early currents were not dependent on the fluence of the photolytic pulse (Fig. 7H) or the amplitude of the early current (Fig. 7I). This result challenges the established idea<sup>31,32,33</sup> that, in mammalian hearts, the termination of Ca<sup>2+</sup> influx through L-type Ca<sup>2+</sup> channels is mostly mediated by Ca<sup>2+</sup> dependent inactivation.

If Ca<sup>2+</sup>-dependent inactivation is not the main mechanism that terminates Ca<sup>2+</sup> influx, in murine hearts during ECC, which is the mechanism? To address this question, we performed experiments to evaluate in which of the AP phases, the Ca<sup>2+</sup> influx that triggers CICR occurs. Interestingly, we found that most of the Ca<sup>2+</sup> current that triggers CICR occurs during phase 1 (Fig. 8A). In order for this to happen, L-type Ca<sup>2+</sup> channels need to be activated at an early stage of the AP (phase 0). Since in phase 0,  $V_m$  moves quickly towards the Ca<sup>2+</sup> electrochemical potential, the amount of Ca<sup>2+</sup> entering into the cells will be very small. At the beginning of phase 1, a fraction of L-type Ca<sup>2+</sup> channels are still open. Thus, throughout phase 1 repolarization, a massive influx of Ca<sup>2+</sup> enters the cells during the deactivation of the Ca<sup>2+</sup> current. This is driven by a rapid increase in the Ca<sup>2+</sup> driving force (Fig. 8A). Finally, when the AP reaches phase 2, the  $V_m$  is negative enough to completely close the L-Type Ca<sup>2+</sup> channels<sup>18</sup>. Thus, this suggests that the influx of Ca<sup>2+</sup> terminates due to voltage-dependent deactivation (in a “tail current” fashion) and not by Ca<sup>2+</sup> dependent inactivation. This phenomenon resembles Ca<sup>2+</sup> entry into the presynaptic terminal during a neuronal AP repolarization to induce neurotransmitter release<sup>34,35,36</sup>. This novel concept alters the currently accepted paradigm in cardiac Ca<sup>2+</sup> signaling.

To further evaluate the idea that Ca<sup>2+</sup> influx triggering Ca<sup>2+</sup> release occurs during phase 1, we performed experiments to change the kinetics of phase 1 repolarization. Phase 1 is a phase of rapid repolarization that is largely governed/caused by the activation of the transient outward current,  $i_{to}$  (Kv. 4.2)<sup>37</sup>. Thus, to slow the repolarization kinetics of phase 1, we partially blocked  $i_{to}$  with 200  $\mu$ M of 4-aminopyridine (4-AP). Fig. 8B and 8C show the nifedipine-sensitive current and the AP recorded simultaneously. 4-AP significantly modified the time course of both the current and the AP repolarization kinetics (Fig. 8D and 8E). Superposition of the nifedipine-sensitive currents before and after 4-AP in Fig. 8F illustrates the dramatic increase in the rapid spike of Ca<sup>2+</sup> current during phase 1, as well as the greater and prolonged inward Na<sup>+</sup> current during phase 2. A summary of several experiments (N=5) is presented in Fig. 8G–H. Slowing down phase 1 increased significantly the time to peak and the half duration of  $i_{early}$  with no significant effect on the amplitude (Fig. 8I). Thus, this result supports the argument that the Ca<sup>2+</sup> influx across the plasma membrane occurs during phase 1.

## DISCUSSION

Although there have been several efforts to record ionic currents in multicellular cardiac preparations, this is the first report of ionic currents recorded in a perfused heart during a physiologically triggered AP. In the early days of the voltage clamp technique, several groups recorded ionic currents in cardiac tissue using the sucrose gap technique<sup>38,39,40,41</sup>.

Even though these pioneering experimental contributions were very important for the advancement of cardiac electrophysiology, these multicellular preparations presented a poor spatial and temporal control of the potential. This limitation was partially overcome by a modification of the cell-attached patch-clamp recording<sup>42</sup>, the loose patch clamp<sup>21,22,43</sup>. This technique has been used to measure ionic currents in multicellular cardiac preparations such as trabeculae and papillary muscle<sup>44,45,46</sup>. However, none of these reports was performed on an intact perfused heart during a physiological triggered AP.

The evaluation of ionic currents during an AP usually has been performed using whole cell AP voltage clamp<sup>47,48,49,50</sup>. With this approach, the AP waveform is first recorded in a particular myocyte under current clamp and then used to voltage clamp different myocytes. Although this approach made it possible to record ionic currents driven by an AP waveform, it does present several drawbacks. For example, as we already mentioned, myocytes from which AP are recorded can come from different regions than the one that will be voltage clamped. In addition, the AP in an isolated cell will be different from one recorded in an intact tissue because neighboring layers of cells can impact the waveform of the local AP. In addition, the study of ionic currents in isolated myocytes is usually done at room temperature and in the presence of a high concentration of intracellular  $\text{Ca}^{2+}$  buffers in order to increase the viability of the isolated myocytes. Under these conditions, it is very unlikely that the time course of the T-tubule potential during an AP voltage clamp will reach the rate of depolarization-repolarization that actually occurs during a physiological AP. This last limitation is mostly defined by the cable properties of the tubular system. In one report where the ionic currents were recorded during a physiological AP<sup>16</sup> in cell-attached configuration on embryonic chick heart cells. Unfortunately, all these recordings were obtained from isolated cells that are electrically, metabolically and mechanically uncoupled from the rest of the tissue, a situation that is highly unphysiological.

Here we introduced a new methodological approach that overcomes most of the experimental problems described above. A unique advantage of LPP is that it made possible the recording of membrane currents during a physiologically triggered AP on an intact perfused heart (Fig. 1). The L-type  $\text{Ca}^{2+}$  channels were selectively re-activated by photo-degrading an antagonist (Fig. 2). The isopotential condition was imposed by the rest of the unphotolyzed area (Fig. 3). The experiments were performed at a quasi-physiological body temperature (33–35 °C) and heart rates (6 Hz). These factors will strongly modify the NCX currents due to the steep temperature dependence ( $Q_{10}$  3.8)<sup>7,48,51,52</sup> and the frequency dependence of  $\text{Ca}^{2+}$  release<sup>51</sup>. The studies reported here using our new approach revealed several unexpected results that alter the existing paradigm of the cardiac AP.

The ionic currents recorded with LPP at the epicardial layer of a perfused heart during an AP showed a fast early component and a slower late component (Fig. 4), which we interpret as L-type  $\text{Ca}^{2+}$  current and NCX current, respectively. The early component is very similar to the one reported by Sah et al<sup>50</sup> using AP voltage clamp. Interestingly, the slower late component is activated by  $\text{Ca}^{2+}$  released from the SR (Fig. 5D and E) and seems to be partially responsible for the genesis of the AP phase 2 (Fig. 5A) recorded in the mouse epicardium<sup>7</sup>. Pharmacological experiments designed to evaluate the molecular basis underlying the early and late component of the nifedipine sensitive currents determined that

the early component was sensitive to  $\text{Cd}^{2+}$  (Fig. 6A and 6B), indicating that this current is mediated by an influx of  $\text{Ca}^{2+}$  through the L-type channel, CaV 1.2. Although  $\text{Cd}^{2+}$  has also a blocking effect on the NCX<sup>52</sup>, the experiments with  $\text{Cd}^{2+}$  were performed in hearts that were pretreated with Ry and Tg (to avoid NCX activation) thus, it is very likely that the currents shown in Fig. 6A and Fig. 6B were not the result of the blocking effect of  $\text{Cd}^{2+}$  on NCX1 but rather on CaV 1.2. Furthermore, the late component was inhibited with micromolar concentrations of the NCX blocker SEA0400 (Fig. 6E and 6F). At this concentration SEA0400 also attenuated the AP phase 2 (Fig. 6C). However, since the amplitude of  $\text{Ca}^{2+}$  transients increased (Fig. 6D), this indicated that the predominant effect of SEA0400 was to inhibit NCX and not the L-type  $\text{Ca}^{2+}$  channels. This result is consistent with experimental findings in transgenic animals by Pott et al<sup>28</sup> showing that NCX was involved in the genesis of AP phase 2. Knock-out of NCX alters the AP waveform and pacemaker activity in SA node cells<sup>53</sup>. Here, we show that electrogenic  $\text{Na}^+$  influx through NCX contributes substantially to prolonging the plateau phase of the AP.

The gain of the CICR process has been defined in recordings from isolated myocytes. In this paper, we showed that LPP can be used to evaluate CICR *ex vivo*. This is a very important parameter to evaluate mechanisms involved in defining cardiac contractility. Fig. 7A–C showed not only that the early inward current was carried by  $\text{Ca}^{2+}$  ions but that increasing the number of available nifedipine sensitive  $\text{Ca}^{2+}$  channels produced an equivalent effect on the amplitude of  $\text{Ca}^{2+}$  currents and  $\text{Ca}^{2+}$  transients. Moreover, the fact that there is a relationship between the late current and the early current (Fig. 7F) indicates that the local gain of CICR can be evaluated in a perfused heart. This last result is very important because it will help to determine the strength of the coupling between  $\text{Ca}^{2+}$  influx and  $\text{Ca}^{2+}$  release in normal and pathological conditions such as ischemia and heart failure. Although it is difficult to make a direct comparison between our data and previous published data due to NCX current-voltage dependency as well as intracellular and extracellular  $\text{Ca}^{2+}$  and  $\text{Na}^+$  concentrations, we found that the magnitude of both the early  $\text{Ca}^{2+}$  current and the late NCX current recorded using LPP (Fig. 7E) are very similar to the ones reported using whole cell voltage clamp in enzymatically isolated mouse ventricular myocytes<sup>28,54,55</sup>.

Another important and unanticipated result was that the decay of  $\text{Ca}^{2+}$  current (early component) does not become faster as the size of the current increases (Fig. 7D). This finding puts some constraints to the general idea that, in all mammalian hearts, the  $\text{Ca}^{2+}$  influx is terminated by  $\text{Ca}^{2+}$ -dependent inactivation. In Fig. 8A we demonstrated that although  $\text{Ca}^{2+}$ -dependent inactivation is not the mechanism involved in the termination of the  $\text{Ca}^{2+}$  influx, the fast  $\text{Ca}^{2+}$  influx terminates. This termination then is due to voltage-dependent deactivation during AP phase 1 repolarization. Thus, although L-type  $\text{Ca}^{2+}$  channels activate during phase 0, most of the  $\text{Ca}^{2+}$  influx occurs during phase 1. Interestingly, it is possible to observe that the early component/peak is composed by a first very fast inward current and a second component/peak that is larger and longer. We think that  $\text{Ca}^{2+}$  is getting into the cell during both peaks. The difference in magnitude can be explained if we consider that most of the  $\text{Ca}^{2+}$  influx through L-type  $\text{Ca}^{2+}$  channels (second peak) occurs during the deactivation of the channels and during the action potential (AP) phase 1. In order for the deactivation to occur, the channels need to open before phase 1 (AP phase 0). This is possible because the AP reaches its peak value in 1 ms and at this point the

driving force for  $\text{Ca}^{2+}$  is highly reduced which could explain the kinetics of the first (fast and short) of the two peaks, which will not contribute significantly to the activation of the ECC process. The concept of  $\text{Ca}^{2+}$  of getting into the cell has been previously suggested in isolated cells by Sah et al<sup>50</sup> and Clark et al<sup>55</sup> but has not been widely accepted. This idea was further explored in Fig. 8 B–H where we changed the rate of phase 1 repolarization by partially blocking  $i_{to}$  with 4-AP. Here, the slowing-down of phase 1 produced a significant prolongation of the time to peak and the half duration of the early  $\text{Ca}^{2+}$  current (Fig. 8 F and H), but not on the current amplitude (Fig. 8 H).

To conclude, LPP allowed the recording of ionic currents from cells electrically and metabolically coupled during their own AP at the intact heart level. Local activation of  $\text{Ca}^{2+}$  currents and/or local increase in myoplasmic  $\text{Ca}^{2+}$  does not have a significant effect on AP repolarization. Nifedipine-sensitive inward current has two components: an  $i_{early}$  that is driven by  $\text{Ca}^{2+}$  influx through L-type  $\text{Ca}^{2+}$  channels and an NCX-dependent  $i_{late}$  component activated by SR  $\text{Ca}^{2+}$  release. Larger L-type  $\text{Ca}^{2+}$  currents do not terminate faster than small ones indicating that  $\text{Ca}^{2+}$ -dependent inactivation is not the main mechanism for current termination during an epicardial AP in mouse ventricle. Finally, the transmembrane  $\text{Ca}^{2+}$  influx that triggers SR  $\text{Ca}^{2+}$  release occurs during phase 1 repolarization in a “tail current” fashion.

Among several possibilities, we think that this mechanism involving an early  $\text{Ca}^{2+}$  influx through the L-type  $\text{Ca}^{2+}$  channels during phase 1 and a late  $\text{Na}^{+}$  influx through the NCX during phase 2 has not been previously described and is now revealed by LPP. This is due to LPP's ability to record ionic currents during an AP in the intact heart, when all the other conductances are active. Consequently, this speeds up the T-tube depolarization and repolarization. In contrast, when AP whole cell voltage clamp is used, only the current of interest is activated and the tubular capacitance and series resistance slow down the kinetics of several ionic currents at the T-tubes. Therefore, the kinetics of  $\text{Ca}^{2+}$  influx to the cell change and subsequently modify the SR  $\text{Ca}^{2+}$  release that activates the NCX current.

In summary, by the use of light-sensitive compounds, LPP is useful for isolation and functional characterization of a particular ionic current from cells mechanically, electrically and metabolically coupled during their own AP at the intact heart level, during health and in disease states.

## Supplementary Material

Refer to Web version on PubMed Central for supplementary material.

## Acknowledgments

We thank Alicia Mattiazzi, Julio Copello, Thomas DeCoursey and Michael Fill for their valuable discussions.

### SOURCES OF FUNDING

This work was supported by grants from American Heart Association (GRNT 7600095 to JRF) and NIH (R01 HL-084487 to ALE; R01 GM-111397 to JRF).

## Nonstandard Abbreviations and Acronyms

<b>LPP</b>	Loose Patch Photolysis
$i_{late}$	late current
$i_{early}$	early current

## REFERENCES

- Higuchi T, Nakaya Y. T wave polarity related to the repolarization process of epicardial and endocardial ventricular surfaces. *Am Heart J.* 1984; 108:290–295. [PubMed: 6464965]
- Woodbury LA, Hecht HH, Christopherson AR. Membrane resting and action potentials of single cardiac muscle fibers of the frog ventricle. *Am J Physiol.* 1951; 164:307–318. [PubMed: 14810936]
- Macfarlane WV. The plateau of the action potential of the frog ventricle. *Circ Res.* 1960; 8:47–56. [PubMed: 14419363]
- Beeler GW, Reuter H. Membrane calcium current in ventricular myocardial fibres. *J Physiol.* 1970; 207:191–209. [PubMed: 5503869]
- Beeler GW, Reuter H. The relation between membrane potential, membrane currents and activation of contraction in ventricular myocardial fibres. *J Physiol.* 1970; 207:211–229. [PubMed: 5503873]
- Reuter H. The dependence of slow inward current in Purkinje fibres on the extracellular calcium-concentration. *J Physiol.* 1967; 192:479–492. [PubMed: 6050160]
- Ferreiro M, Petrosky AD, Escobar AL. Intracellular  $Ca^{2+}$  release underlies the development of phase 2 in mouse ventricular action potentials. *Am J Physiol Heart Circ Physiol.* 2012; 302:H1160–H1172. [PubMed: 22198177]
- Antzelevitch C, Fish J. Electrical heterogeneity within the ventricular wall. *Basic Res Cardiol.* 2001; 96:517–527. [PubMed: 11770069]
- Gómez AM, Benitah JP, Henzel D, Vinet A, Lorente P, Delgado C. Modulation of electrical heterogeneity by compensated hypertrophy in rat left ventricle. *Am J Physiol.* 1997; 272:H1078–H1086. [PubMed: 9087578]
- Emori T, Antzelevitch C. Cellular basis for complex T waves and arrhythmic activity following combined  $I_{Kr}$  and  $I_{Ks}$  block. *J Cardiovasc Electrophysiol.* 2001; 12:1369–1378. [PubMed: 11797994]
- Yan GX, Antzelevitch C. Cellular basis for the electrocardiographic J wave. *Circulation.* 1996; 93:372–379. [PubMed: 8548912]
- Yan GX, Shimizu W, Antzelevitch C. Characteristics and distribution of M cells in arterially perfused canine left ventricular wedge preparations. *Circulation.* 1998; 98:1921–1927. [PubMed: 9799214]
- Rosati B, Pan Z, Lypen S, Wang HS, Cohen I, Dixon JE, McKinnon D. Regulation of KChIP2 potassium channel beta subunit gene expression underlies the gradient of transient outward current in canine and human ventricle. *J Physiol.* 2001; 533:119–125. [PubMed: 11351020]
- Calloe K, Soltysinska E, Jespersen T, Lundby A, Antzelevitch C, Olesen S-P, Cordeiro JM. Differential effects of the transient outward  $K^+$  current activator NS5806 in the canine left ventricle. *J Mol Cell Cardiol.* 2010; 48:191–200. [PubMed: 19632239]
- Apkon M, Nerbonne JM. Characterization of two distinct depolarization-activated  $K^+$  currents in isolated adult rat ventricular myocytes. *J Gen Physiol.* 1991; 97:973–1011. [PubMed: 1865177]
- Fischmeister R, DeFelice LJ, Ayer RK, Levi R, DeHaan RL. Channel currents during spontaneous action potentials in embryonic chick heart cells. The action potential patch clamp. *Biophys J.* 1984; 46:267–271. [PubMed: 6089925]
- Banyasz T, Horvath B, Jian Z, Izu LT, Chen-Izu Y. Profile of L-type  $Ca^{2+}$  current and  $Na^+/Ca^{2+}$  exchange current during cardiac action potential in ventricular myocytes. *Heart Rhythm Off J Heart Rhythm Soc.* 2012; 9:134–142.



18. Santana LF, Kranias EG, Lederer WJ. Calcium sparks and excitation-contraction coupling in phospholamban-deficient mouse ventricular myocytes. *J Physiol.* 1997; 503(Pt 1):21–29. [PubMed: 9288671]
19. Mejía-Alvarez R, Manno C, Villalba-Galea CA, del Valle Fernández L, Costa RR, Fill M, Gharbi T, Escobar AL. Pulsed local-field fluorescence microscopy: a new approach for measuring cellular signals in the beating heart. *Pflüg Arch Eur J Physiol.* 2003; 445:747–758.
20. Kornyejev D, Reyes M, Escobar AL. Luminal  $\text{Ca}^{2+}$  content regulates intracellular  $\text{Ca}^{2+}$  release in subepicardial myocytes of intact beating mouse hearts: effect of exogenous buffers. *Am J Physiol Heart Circ Physiol.* 2010; 298:H2138–H2153. [PubMed: 20382849]
21. Almers W, Roberts WM, Ruff RL. Voltage clamp of rat and human skeletal muscle: measurements with an improved loose-patch technique. *J Physiol.* 1984; 347:751–768. [PubMed: 6323705]
22. Roberts WM, Almers W. An improved loose patch voltage clamp method using concentric pipettes. *Pflüg Arch Eur J Physiol.* 1984; 402:190–196.
23. Escobar AL, Perez CG, Reyes ME, Lucero SG, Kornyejev D, Mejía-Alvarez R, Ramos-Franco J. Role of inositol 1,4,5-trisphosphate in the regulation of ventricular  $\text{Ca}^{2+}$  signaling in intact mouse heart. *J Mol Cell Cardiol.* 2012; 53:768–779. [PubMed: 22960455]
24. Sanchez JA, Vergara J. Modulation of  $\text{Ca}^{2+}$  transients by photorelease of caged nucleotides in frog skeletal muscle fibers. *Am J Physiol.* 1994; 266:C1291–C1300. [PubMed: 8203494]
25. Escobar AL, Velez P, Kim AM, Cifuentes F, Fill M, Vergara JL. Kinetic properties of DM-nitrophen and calcium indicators: rapid transient response to flash photolysis. *Pflüg Arch Eur J Physiol.* 1997; 434:615–631.
26. Gurney AM, Nerbonne JM, Lester HA. Photoinduced removal of nifedipine reveals mechanisms of calcium antagonist action on single heart cells. *J Gen Physiol.* 1985; 86:353–379. [PubMed: 2414392]
27. Morad M, Goldman YE, Trentham DR. Rapid photochemical inactivation of  $\text{Ca}^{2+}$ -antagonists shows that  $\text{Ca}^{2+}$  entry directly activates contraction in frog heart. *Nature.* 1983; 304:635–638. [PubMed: 6308474]
28. Pott C, Philipson KD, Goldhaber JI. Excitation-contraction coupling in  $\text{Na}^{+}$ - $\text{Ca}^{2+}$  exchanger knockout mice: reduced transsarcolemmal  $\text{Ca}^{2+}$  flux. *Circ Res.* 2005; 97:1288–1295. [PubMed: 16293789]
29. Tanaka H, Nishimaru K, Aikawa T, Hirayama W, Tanaka Y, Shigenobu K. Effect of SEA0400, a novel inhibitor of sodium-calcium exchanger, on myocardial ionic currents. *Br J Pharmacol.* 2002; 135:1096–1100. [PubMed: 11877314]
30. Tanaka H, Namekata I, Takeda K, Kazama A, Shimizu Y, Moriwaki R, Hirayama W, Sato A, Kawanishi T, Shigenobu K. Unique excitation-contraction characteristics of mouse myocardium as revealed by SEA0400, a specific inhibitor of  $\text{Na}^{+}$ - $\text{Ca}^{2+}$  exchanger. *Naunyn Schmiedebergs Arch Pharmacol.* 2005; 371:526–534. [PubMed: 16003546]
31. Peterson BZ, DeMaria CD, Adelman JP, Yue DT. Calmodulin is the  $\text{Ca}^{2+}$  sensor for  $\text{Ca}^{2+}$ -dependent inactivation of L-type calcium channels. *Neuron.* 1999; 22:549–558. [PubMed: 10197534]
32. Bers DM, Perez-Reyes E. Ca channels in cardiac myocytes: structure and function in  $\text{Ca}^{2+}$  influx and intracellular Ca release. *Cardiovasc Res.* 1999; 42:339–360. [PubMed: 10533572]
33. Greenstein JL, Winslow RL. An integrative model of the cardiac ventricular myocyte incorporating local control of  $\text{Ca}^{2+}$  release. *Biophys J.* 2002; 83:2918–2945. [PubMed: 12496068]
34. Llinás R, Steinberg IZ, Walton K. Relationship between presynaptic calcium current and postsynaptic potential in squid giant synapse. *Biophys J.* 1981; 33:323–351. [PubMed: 6261850]
35. Yazejian B, DiGregorio DA, Vergara JL, Poage RE, Meriney SD, Grinnell AD. Direct measurements of presynaptic calcium and calcium-activated potassium currents regulating neurotransmitter release at cultured *Xenopus* nerve-muscle synapses. *J Neurosci Off J Soc Neurosci.* 1997; 17:2990–3001.
36. Pattillo JM, Yazejian B, DiGregorio DA, Vergara JL, Grinnell AD, Meriney SD. Contribution of presynaptic calcium-activated potassium currents to transmitter release regulation in cultured *Xenopus* nerve-muscle synapses. *Neuroscience.* 2001; 102:229–240. [PubMed: 11226687]



37. Guo W, Xu H, London B, Nerbonne JM. Molecular basis of transient outward  $K^+$  current diversity in mouse ventricular myocytes. *J Physiol.* 1999; 521(Pt 3):587–599. [PubMed: 10601491]
38. Beeler GW, Reuter H. Voltage clamp experiments on ventricular myocardial fibres. *J Physiol.* 1970; 207:165–190. [PubMed: 5503866]
39. Trautwein W, McDonald TF. Current-voltage relations in ventricular muscle preparations from different species. *Pflüg Arch Eur J Physiol.* 1978; 374:79–89.
40. Giebisch G, Weidmann S. Membrane currents in mammalian ventricular heart muscle fibers using a voltage-clamp technique. *J Gen Physiol.* 1971; 57:290–296. [PubMed: 5544795]
41. Tung L, Morad M. A comparative electrophysiological study of enzymatically isolated single cells and strips of frog ventricle. *Pflüg Arch Eur J Physiol.* 1985; 405:274–284.
42. Hamill OP, Marty A, Neher E, Sakmann B, Sigworth FJ. Improved patch-clamp techniques for high-resolution current recording from cells and cell-free membrane patches. *Pflüg Arch Eur J Physiol.* 1981; 391:85–100.
43. Perkins KL. Cell-attached voltage-clamp and current-clamp recording and stimulation techniques in brain slices. *J Neurosci Methods.* 2006; 154:1–18. [PubMed: 16554092]
44. Antoni H, Böcker D, Eickhorn R. Sodium current kinetics in intact rat papillary muscle: measurements with the loose-patch-clamp technique. *J Physiol.* 1988; 406:199–213. [PubMed: 2855435]
45. Eickhorn R, Dräger C, Antoni H. Influence of cell isolation and recording technique on the voltage dependence of the fast cardiac sodium current of the rat. *J Mol Cell Cardiol.* 1994; 26:1095–1108. [PubMed: 7799448]
46. Kirstein M, Eickhorn R, Kochsiek K, Langenfeld H. Dose-dependent alteration of rat cardiac sodium current by isoproterenol: results from direct measurements on multicellular preparations. *Pflüg Arch Eur J Physiol.* 1996; 431:395–401.
47. Nuss HB, Marban E. Electrophysiological properties of neonatal mouse cardiac myocytes in primary culture. *J Physiol.* 1994; 479(Pt 2):265–279. [PubMed: 7799226]
48. Yuan W, Ginsburg KS, Bers DM. Comparison of sarcolemmal calcium channel current in rabbit and rat ventricular myocytes. *J Physiol.* 1996; 493(Pt 3):733–746. [PubMed: 8799895]
49. Arreola J, Dirksen RT, Shieh RC, Williford DJ, Sheu SS.  $Ca^{2+}$  current and  $Ca^{2+}$  transients under action potential clamp in guinea pig ventricular myocytes. *Am J Physiol.* 1991; 261:C393–C397. [PubMed: 1651654]
50. Sah R, Ramirez RJ, Backx PH. Modulation of  $Ca^{2+}$  release in cardiac myocytes by changes in repolarization rate: role of phase-1 action potential repolarization in excitation-contraction coupling. *Circ Res.* 2002; 90:165–173. [PubMed: 11834709]
51. Blaustein MP, Lederer WJ. Sodium/calcium exchange: its physiological implications. *Physiol Rev.* 1999; 79:763–854. [PubMed: 10390518]
52. Bersohn MM, Vemuri R, Schuil DW, Weiss RS, Philipson KD. Effect of temperature on sodium-calcium exchange in sarcolemma from mammalian and amphibian hearts. *Biochim Biophys Acta.* 1991; 1062:19–23. [PubMed: 1998706]
53. Kornyejev D, Petrosky AD, Zepeda B, Ferreiro M, Knollmann B, Escobar AL. Calsequestrin 2 deletion shortens the refractoriness of  $Ca^{2+}$  release and reduces rate-dependent  $Ca^{2+}$ -alternans in intact mouse hearts. *J Mol Cell Cardiol.* 2012; 52:21–31. [PubMed: 21983287]
54. Torrente AG, Zhang R, Zaini A, Giani JF, Kang J, Lamp ST, Philipson KD, Goldhaber JJ. Burst pacemaker activity of the sinoatrial node in sodium-calcium exchanger knockout mice. *Proc Natl Acad Sci USA.* 2015; 112:9769–9774. [PubMed: 26195795]
55. Clark RB, Bouchard RA, Giles WR. Action potential duration modulates calcium influx,  $Na^+$ - $Ca^{2+}$  exchange, and intracellular calcium release in rat ventricular myocytes. *Ann N Y Acad Sci.* 1996; 779:417–429. [PubMed: 8659858]

## Novelty and Significance

### What Is Known?

- Ventricular ionic currents are usually recorded from enzymatically-dissociated cells by voltage clamping.
- Phase 2 of the action potential is driven by  $\text{Ca}^{2+}$  influx through L-type channels.
- During an action potential, the L-type  $\text{Ca}^{2+}$  current is terminated by a  $\text{Ca}^{2+}$ -dependent inactivation mechanism.

### What New Information Does This Article Contribute?

- We measured ionic currents in intact hearts under physiological AP.
- The  $\text{Ca}^{2+}$  influx that triggers  $\text{Ca}^{2+}$  release occurs during phase 1 (not phase 2) of the action potential while the activation of  $\text{Na}^+/\text{Ca}^{2+}$  exchanger (NCX) forward current drives phase 2.
- Current through L-type  $\text{Ca}^{2+}$  channel is terminated by voltage-dependent deactivation.

Ventricular myocytes are electrically and metabolically coupled. These couplings determine the electrical properties of the heart. Unfortunately, these currents are usually measured in isolated myocytes, which differ significantly in their properties from the functional syncytium. In the intact heart, the electrical and metabolic status will determine the key mechanisms involved in action potential generation. Here, using the intact heart, we recorded ionic currents underlying the action potential. Our approach revealed that the  $\text{Ca}^{2+}$  influx through L-type  $\text{Ca}^{2+}$  channels that triggers SR  $\text{Ca}^{2+}$  release occurs during phase 1, while phase 2 results from NCX activity. These findings suggest that the mouse epicardial action potential is different from other reported ventricular APs, where the activity of L-type channels has been indicated as being responsible for phase 2 of the action potential. Moreover, our findings also indicate that  $\text{Ca}^{2+}$ -dependent inactivation is not the central mechanism for current termination during action potential. This approach will help to address questions that can only be evaluated on functional hearts providing a bridge between classical electrophysiological studies and cardiac function under normal and pathological conditions.

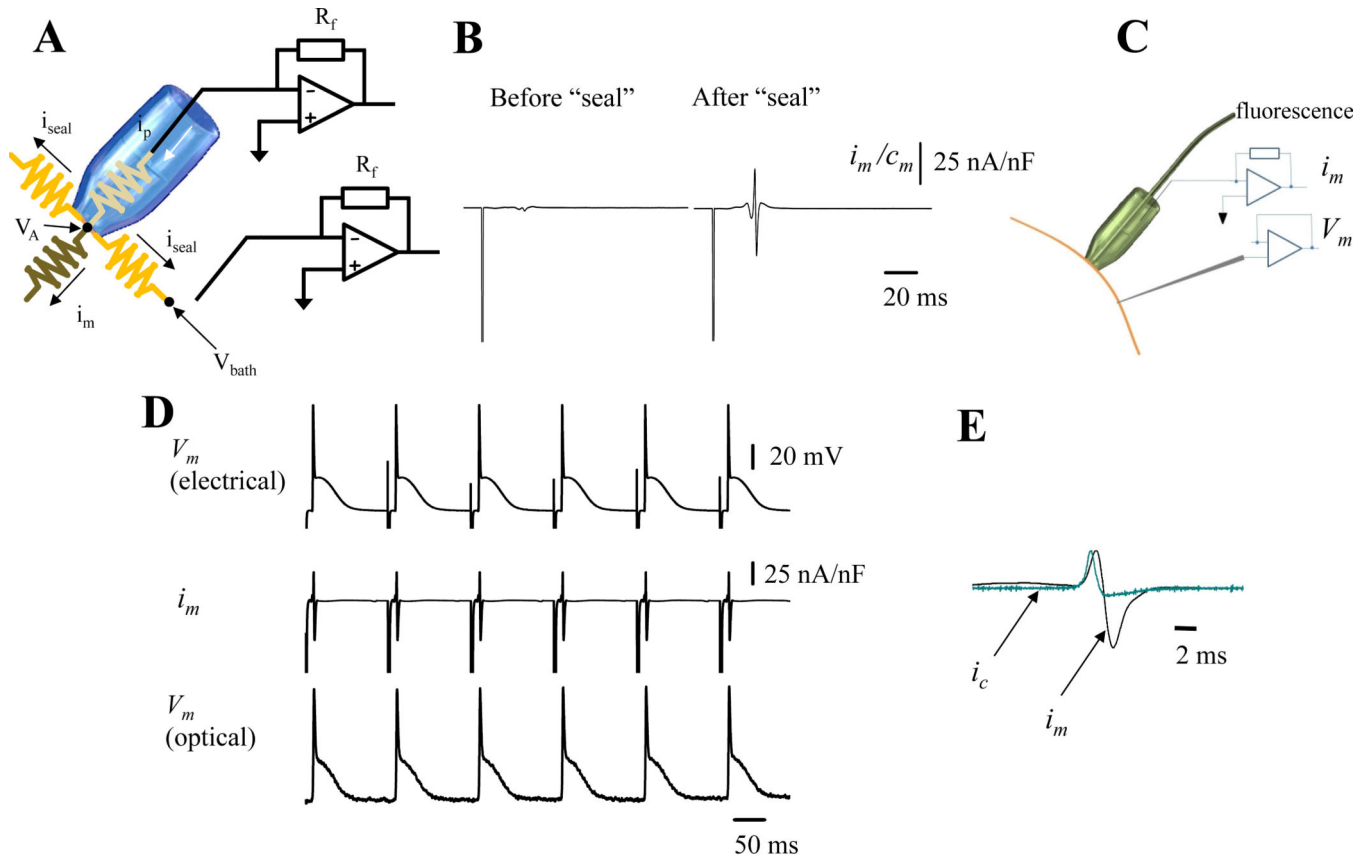


**Figure 1. Recording transmembrane currents on epicardium**

**A.** An electrical scheme of the loose patch recording circuit. The bath and the interior of the pipette are clamped at the same potential. A second current to voltage converter sets the bath potential and acts as a guard to electrically increase the seal resistance. For more detailed information see Online Figure I **B.** Traces show the extracellularly recorded currents before and after the seal. Both recordings show a spike produced by the electrical stimulus applied at the apex of the heart to pace the organ. However, only the recordings obtained after the seal was applied show the membrane current during an AP. **C.** Scheme of the LPP arrangement showing a giant patch for measuring  $i_m$ , the intracellular microelectrode for electrically recording  $V_m$  and an PLFFM optical fiber positioned inside the giant pipette to optically record  $V_m$  optically. **D.** Electrical and optical recordings obtained from the epicardial layer of a mouse heart loaded with the potentiometric dye Di-8-ANNEPS and extracellularly paced at 6 Hz. **E.** Simultaneous recordings of the membrane current  $i_m$  (black) and the calculated capacitive current  $i_c$  (teal).  $i_m$  is the summation of all the ionic currents plus the capacitive current under the patch. (n= 6 hearts).

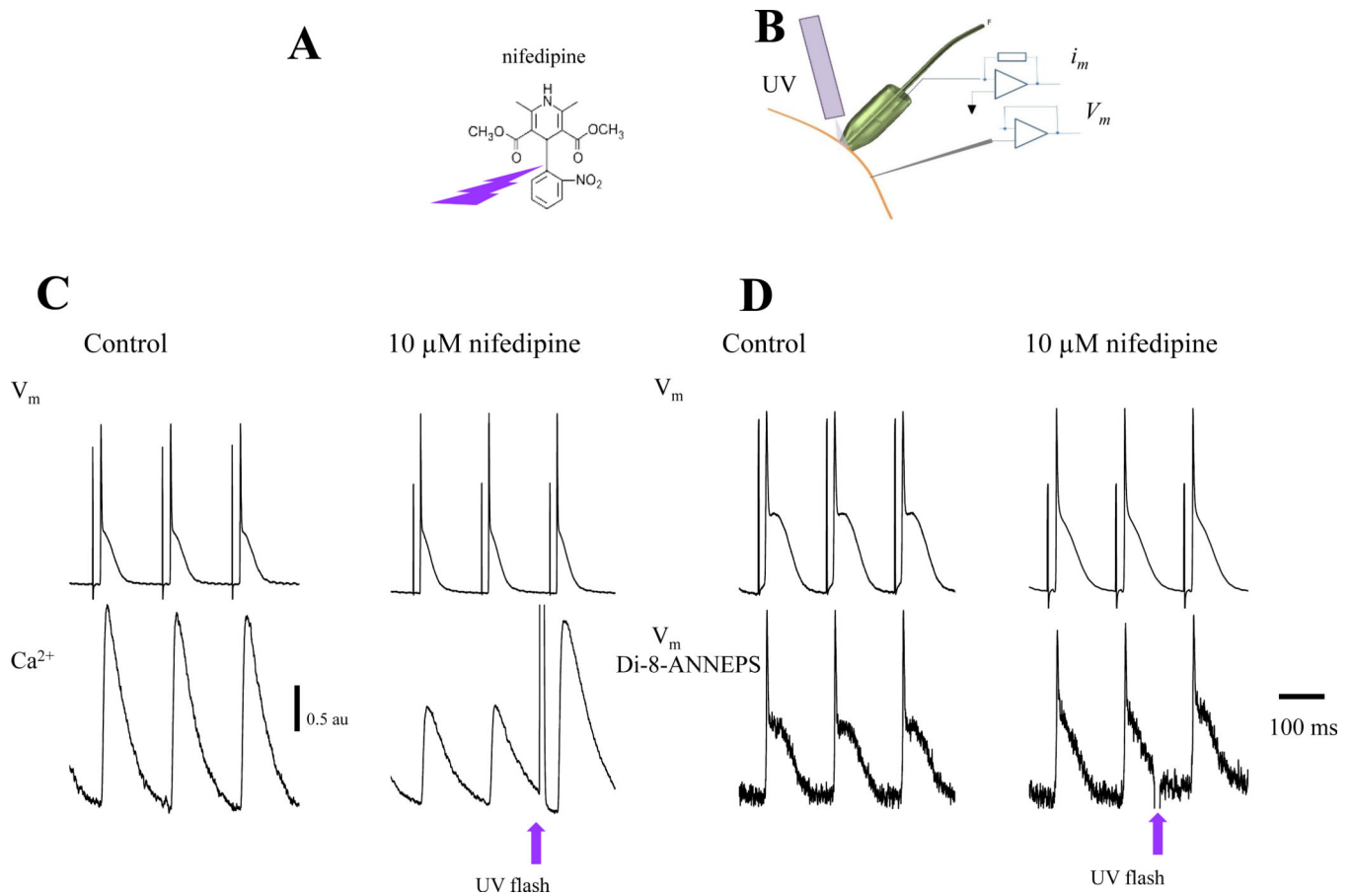


**Figure 2. Nifedipine blocking action removed by UV photolysis**

**A.** Scheme of nifedipine photo-breakdown. Nifedipine, like some other dihydropyridines, contains an O-nitrobenzyl moiety that confers their photolability. The photolytic product no longer inhibits L-type  $\text{Ca}^{2+}$  current<sup>26,27</sup>. **B.** Experimental arrangement to measure  $\text{Ca}^{2+}$  or  $V_m$  using fluorescent dyes and electrical  $V_m$  by means of an intracellular microelectrode while applying UV pulses through an additional quartz multimode optical fiber. **C.** Simultaneous recordings of APs with an intracellular microelectrode and  $\text{Ca}^{2+}$  transients with Rhod-2 AM, before and after the perfusion of 10  $\mu\text{M}$  nifedipine. Nifedipine reduced the amplitude of  $\text{Ca}^{2+}$  transients and the duration of AP. Upon illumination (UV flash), the breakdown of nifedipine occurs relieving the inhibition of L-type  $\text{Ca}^{2+}$  channels allowing an increase in the influx of  $\text{Ca}^{2+}$  that promotes a larger release from the SR as illustrated in the bottom panel. Similar results were obtained in 10 hearts. **D.** Concurrent electrical and optical recordings of AP in hearts loaded with Di-8-ANNEPS. Nifedipine induced a shortening of AP duration. However, nifedipine photolysis had no significant effect on the time course of APs ( $n=6$  hearts).

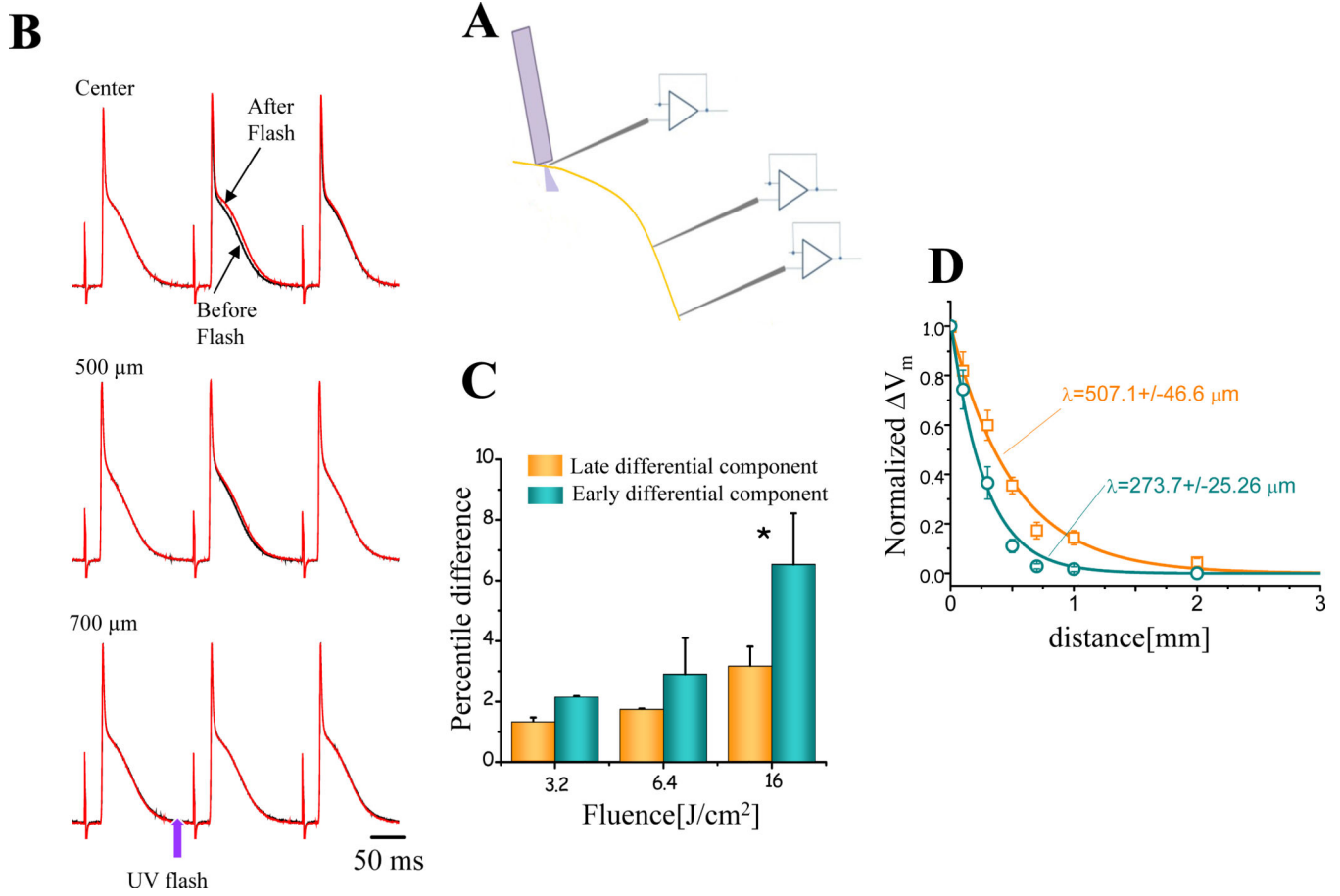


**Figure 3. Testing the electrotonic coupling between tissue neighboring the recording area**  
**A.** Scheme of the experiment. The microelectrode was positioned at different distances from the photolysis fiber. **B.** AP traces recorded at the indicated distances from the photolysis site, before (black traces) and after (red traces) the UV flash. The flash intensity (“fluence”) used for these records was 6.5 J/cm<sup>2</sup>. **C.** Effect of nifedipine photolysis effect on the AP repolarization. Two consecutive AP traces (before and after the flash at the photolysis site) were subtracted. The differential records obtained at increasing photolysis fluences (density of energy) display an early and a late differential component. The early and late components of this difference correspond to changes in AP phase 1 and 2, respectively. The percentile difference between the early and the late component (n=5 hearts) were calculated using the

formula  $\left| \frac{Vm_{\text{before flash}} - Vm_{\text{after flash}}}{Vm_{\text{before flash}}} \right| \times 100$ . **D.** Spatial distribution of the photolysis induced changes in the early and late differential component of the membrane potential at different distances from the photolysis site. Teal corresponds to the early differential component, while the orange to the late differential component. The data were fitted with the spatial

component of a cable equation:  $\frac{Vm(x)}{Vm(0)} = e^{-\frac{x}{\lambda}}$ .

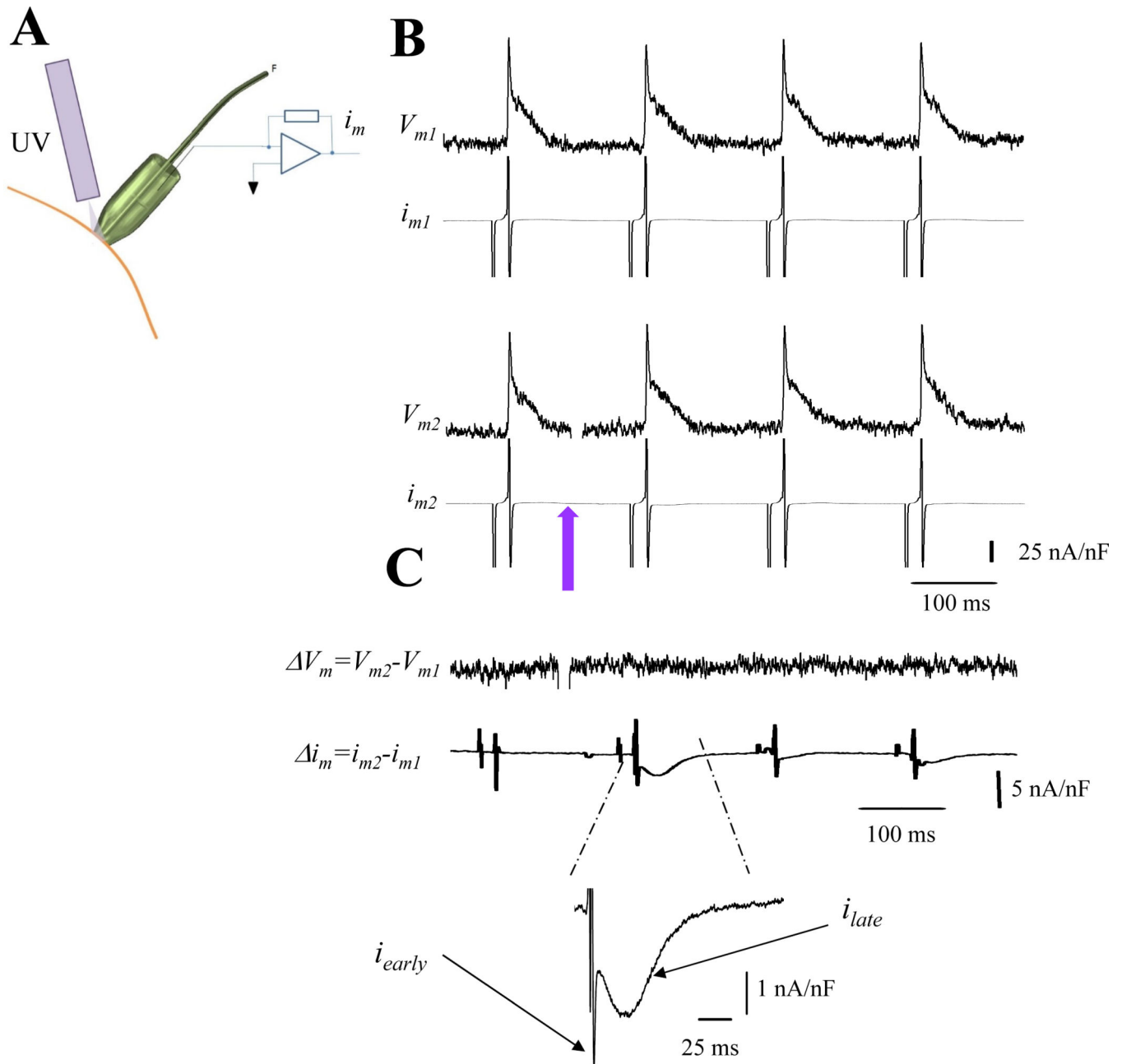


**Figure 4. Dissecting ionic currents during triggered AP**

**A.** Experimental arrangement to measure optically  $V_m$  and electrically  $i_m$  during photolysis.

**B.** Traces of APs and  $i_m$  in the presence of 10  $\mu$ M nifedipine. Upper and lower records (e.g.,  $V_{m1}$  and  $i_{m1}$  and  $V_{m2}$  and  $i_{m2}$ ) were recorded under identical conditions in the same location. The violet arrow indicates the time when nifedipine was photolyzed (traces  $V_{m2}$  and  $i_{m2}$ ).

**C.** Difference between  $V_{m2} - V_{m1}$  ( $V_m$ ) and  $i_{m2} - i_{m1}$  ( $i_m$ ). No changes were observed in the differential trace ( $V_m$ ) after nifedipine photolysis. However, the subtraction  $i_{m2} - i_{m1}$  revealed a nifedipine sensitive current that displays an early fast component and a slower late component (n= 6 hearts).

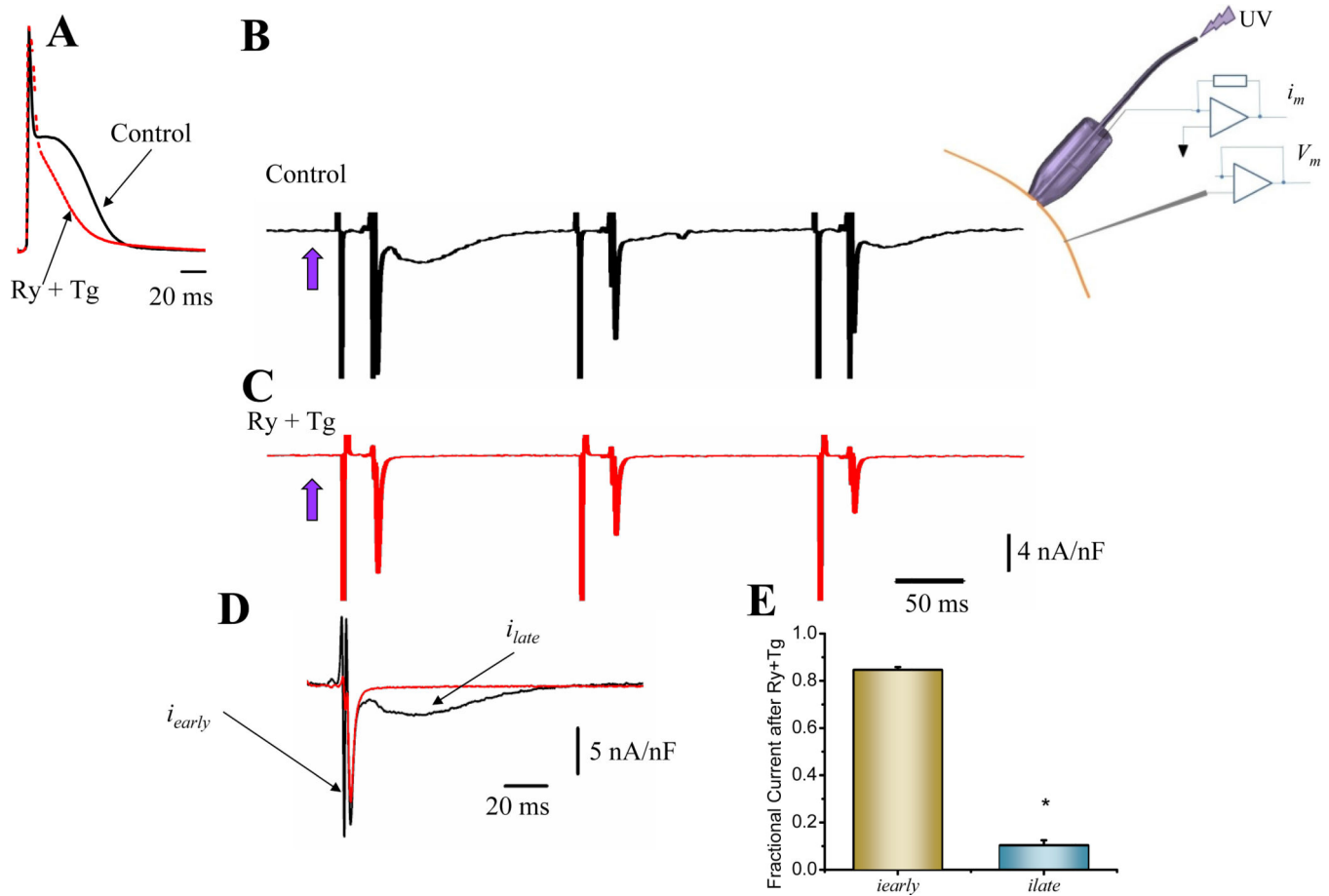


### Figure 5. Ionic currents underlying action potential phase 2

**A.** Effect of Ry (10  $\mu$ M) and Tg (2  $\mu$ M) perfusion on epicardial APs. The treatment had a strong effect impairing the development of AP phase 2 (n=18 hearts). **B.** Differential ionic current after photolysis (violet arrow) of 10  $\mu$ M nifedipine (control) (n=22 hearts). **C.** Differential ionic current in a heart perfused with Ry and Tg (n=9 hearts). **D.** Comparison of ionic current traces in absence and in presence of Ry and Tg. **E.** Histogram showing that the late component  $i_{late}$  is highly inhibited by Ry and Tg whereas the early  $i_{early}$  is mostly unaffected (n=5 p<0.02).



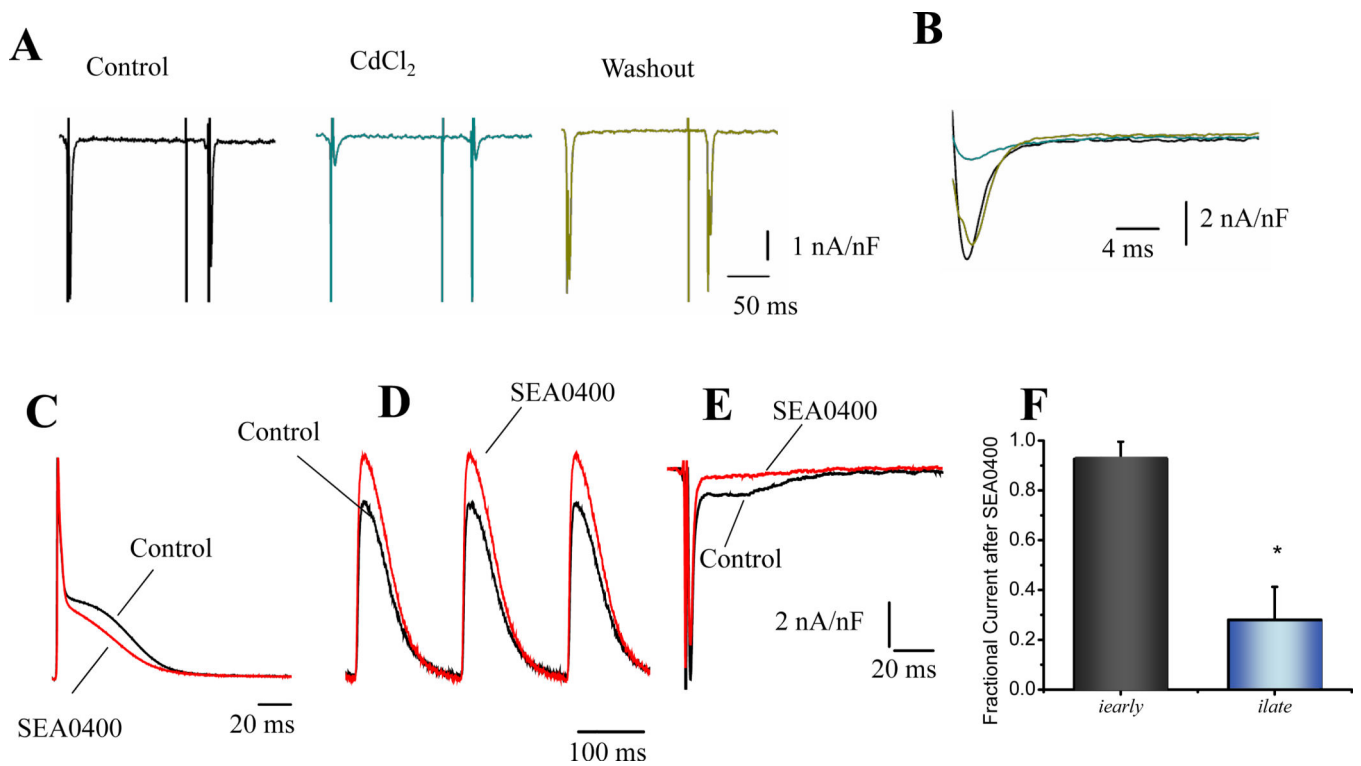


**Figure 6. Probing the molecular nature of the differential ionic currents**

**A.** 100 μM CdCl<sub>2</sub> was able to block the fast component (*i<sub>early</sub>*), in a reversible manner (n=3 hearts). **B.** Comparison of the amplitude and kinetics of *i<sub>early</sub>* during CdCl<sub>2</sub> treatment. **C.** Effect of 10 μM SEA0400 on epicardial APs. SEA0400 is a potent blocker of NCX and had a similar effect as Ry and Tg treatment on the AP repolarization (n=6 hearts). **D.** Effect of SEA0400 on the amplitude of epicardial Ca<sup>2+</sup> transients. As expected, NCX's block induced an increase in the Ca<sup>2+</sup> transient amplitude (n=3 hearts). **E.** Effect of SEA0400 on the photolytically activated ionic currents (n=3 hearts). **F.** Histogram showing that SEA0400 had a selective effect on *i<sub>late</sub>* indicating that in mouse epicardium, an NCX current activated by SR Ca<sup>2+</sup> release is involved in the genesis of AP phase 2. \* Populations means are significantly different at a level of 0.05 (ANOVA).

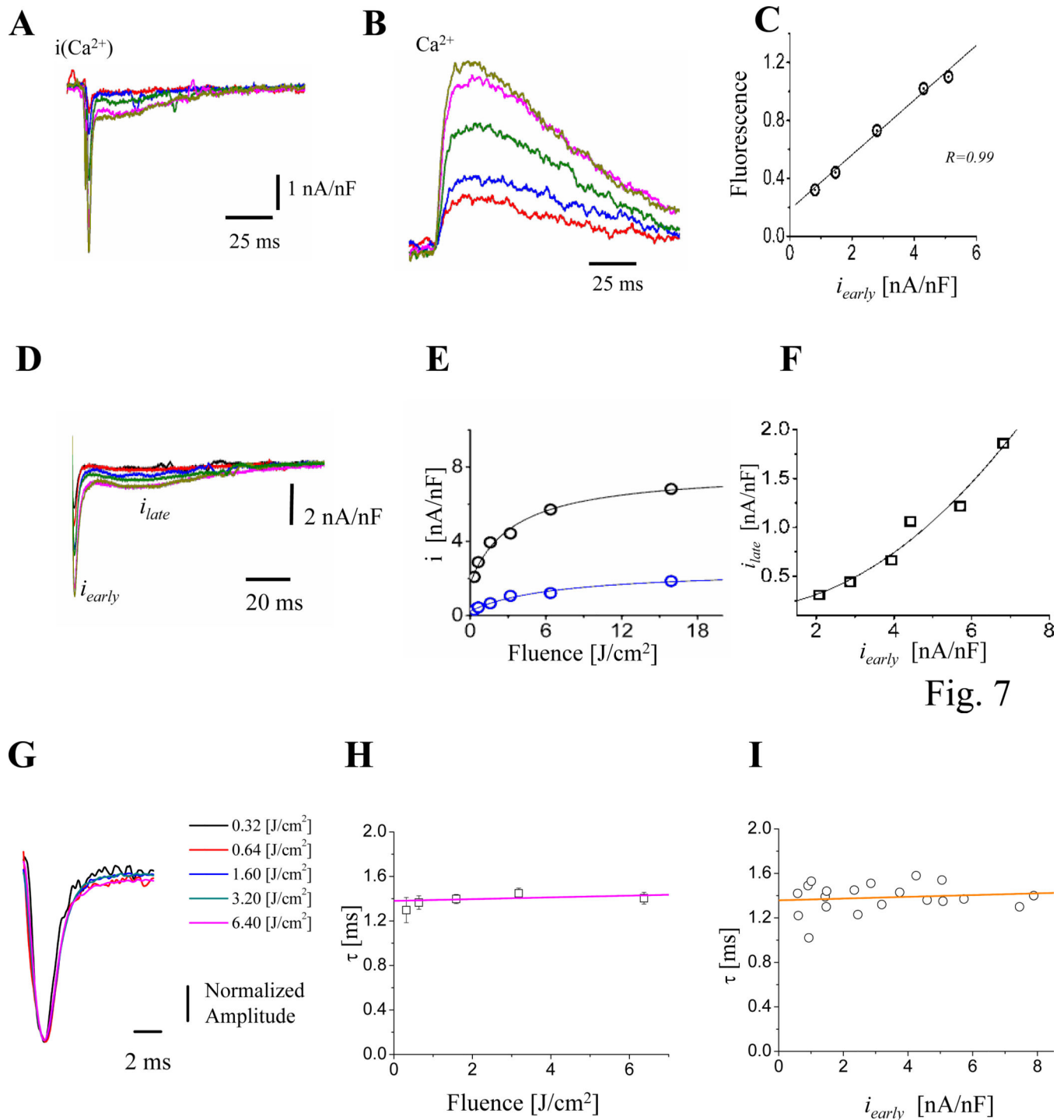


Fig. 7

**Figure 7. Testing the gain of CICR at the intact heart level**

**A.** Ionic currents during triggered APs illustrating the effects of varying the fraction of nifedipine broken down by applying UV pulses of different energies. Similar results were obtained in 6 hearts. **B.**  $\text{Ca}^{2+}$  transients, measured with X-Rhod-5F AM, recorded simultaneously at the same location where the ionic currents (panel A) were obtained. The colors of the fluorescent traces correspond to the LPP currents. **C.** Relationship between

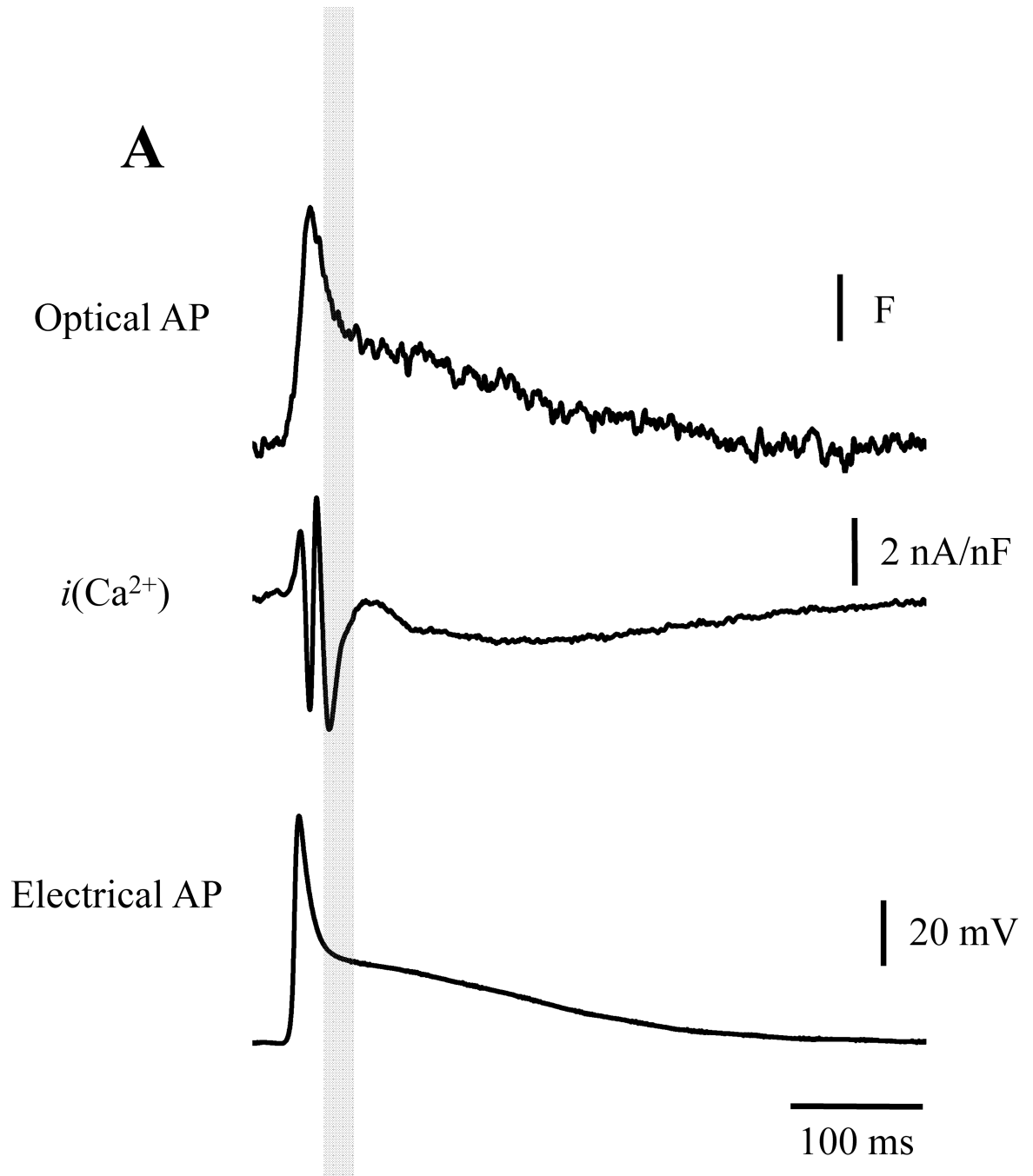
Ca<sup>2+</sup> transients amplitude and  $i_{early}$ . There is a direct relationship between intracellular Ca<sup>2+</sup> and the Ca<sup>2+</sup> influx (n=3 hearts). **D.** Ionic current traces obtained with different flash energies in hearts not perfused with exogenous Ca<sup>2+</sup> indicators. **E.** Fluence dependency of  $i_{late}$  (blue) and  $i_{early}$  (black), both current components saturate for high fluences indicating that at these energies all nifedipine molecules were locally broken down. **F.** Nonlinear relationship between  $i_{late}$  and  $i_{early}$  (n=15 hearts). **G.** Time courses of normalized early currents recorded at different fluences. **H.** Relaxation time constants of the early currents as function of the photolysis fluence. **I.** Relaxation time constants of the early currents as function of the peak early current amplitude. (n= 4 hearts).

Author Manuscript

Author Manuscript

Author Manuscript

Author Manuscript



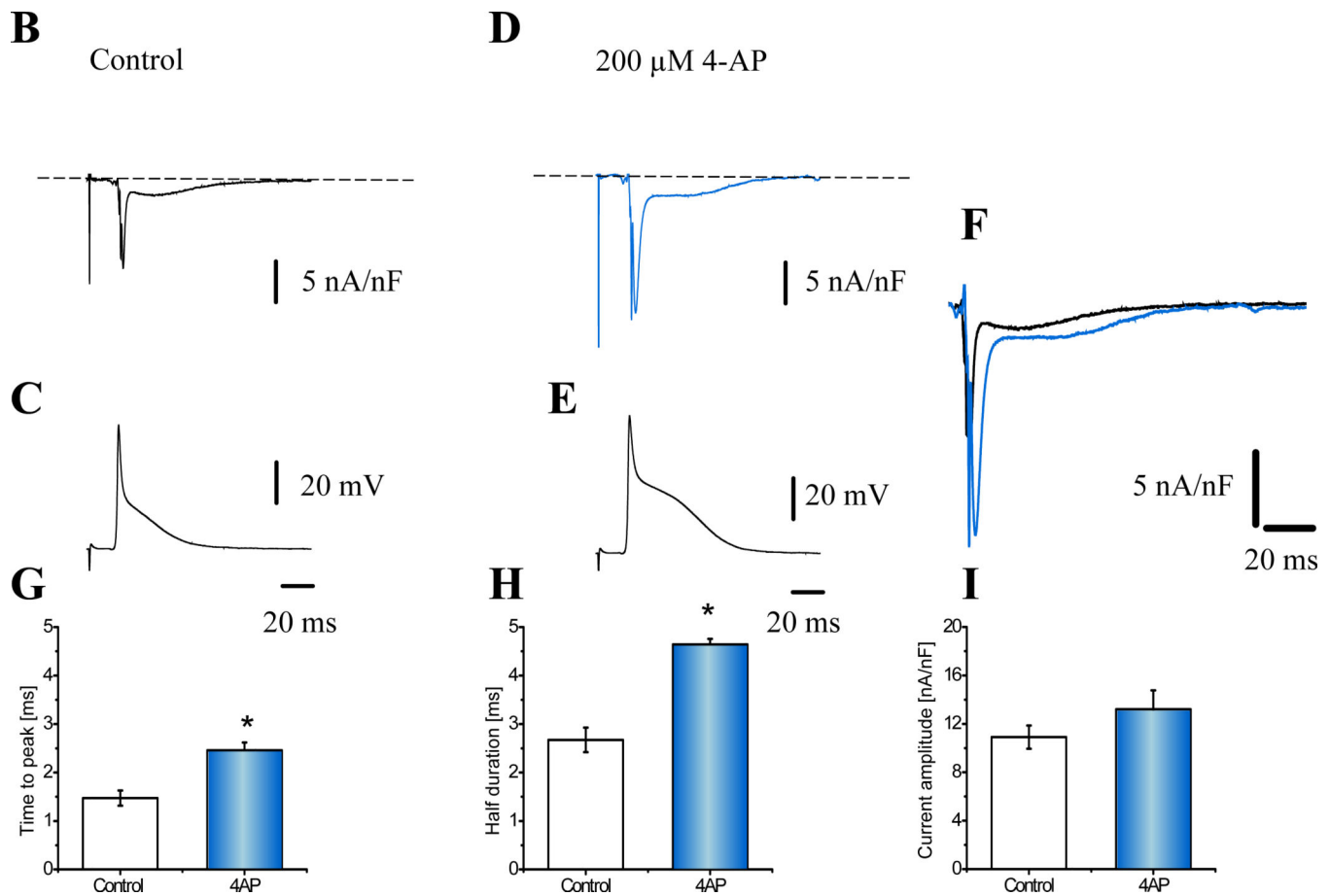


**Figure 8. Defining the action potential phase of calcium entry into the cell**

**A.** The maximum influx of  $\text{Ca}^{2+}$  occurs during phase-I repolarization indicating that  $\text{Ca}^{2+}$  is entering the myocytes in a “tail current” fashion ( $n=6$  hearts) and that  $\text{Ca}^{2+}$  influx terminates because of a voltage dependent deactivation. **B.** Nifedipine sensitive currents during the corresponding AP (**C.**). **D.** and **E.** Illustrate the effect of 200  $\mu$ M 4-AP. **F.** A comparison of the ionic currents before (black) and after 4-AP (blue). Panels **G.**–**I.** Histograms illustrating the effect of 4-AP on the ionic current kinetics and amplitude ( $n=4$  Hearts). \*Populations means are significantly different at a level of 0.05 (ANOVA).